

CP Violation in Kaon Decays (II)

Taku Yamanaka, *Osaka University*

To appear in the proceedings of the 50 years of CP violation conference, 10 – 11 July, 2014, held at Queen Mary University of London, UK.

1 Introduction

Major progress has been made in kaon physics in the past 50 years. The number of observed $K_L \rightarrow \pi^+\pi^-$ events has increased by 6 orders of magnitude, and the observed CP violation was experimentally proven to be caused by a complex phase in the CKM matrix. This mechanism is now a fundamental piece of the standard model. Recent kaon experiments are now even searching for new physics *beyond* the standard model with $K \rightarrow \pi\nu\bar{\nu}$ decays. The branching ratios of $K \rightarrow \pi\nu\bar{\nu}$ decays are 7–8 orders of magnitude smaller than the branching ratio of $K_L \rightarrow \pi^+\pi^-$, and CP -violating $K_L \rightarrow \pi^0\pi^0$ decay is now a major background for $K_L \rightarrow \pi^0\nu\bar{\nu}$ experiments.

This paper reviews the progress of kaon experiments in the US and Japan as requested by the conference organizer, and how the 6–7 orders of magnitude improvements were possible in the past 50 years.¹

2 Quest for ϵ'/ϵ

Soon after the discovery of CP violation [1], the $K_L \rightarrow \pi^+\pi^-$ decay was explained to be caused by an admixture of a CP -even component in the K_L [2]:

$$|K_L\rangle \sim |K_{odd}\rangle + \epsilon|K_{even}\rangle, \quad (1)$$

where this CP -even component was decaying to a CP -even $\pi^+\pi^-$ state. This admixture is introduced by a complex phase in the $K^0 - \bar{K}^0$ mixing. The next question was whether the CP -odd K_{odd} can directly decay to a CP -even $\pi\pi$ state. Such process is called *direct CP* violation. If the direct CP violation exists, the ratios between decay amplitudes:

$$\eta_{\pm} \equiv A(K_L \rightarrow \pi^+\pi^-)/A(K_S \rightarrow \pi^+\pi^-) = \epsilon + \epsilon' \quad \text{and} \quad (2)$$

$$\eta_{00} \equiv A(K_L \rightarrow \pi^0\pi^0)/A(K_S \rightarrow \pi^0\pi^0) = \epsilon - 2\epsilon' \quad (3)$$

can be different due to isospin. The existence of the direct CP violation can thus be tested by checking whether the double ratio:

$$R \equiv \frac{BR(K_L \rightarrow \pi^+\pi^-)/BR(K_S \rightarrow \pi^+\pi^-)}{BR(K_L \rightarrow \pi^0\pi^0)/BR(K_S \rightarrow \pi^0\pi^0)} \quad (4)$$

$$= \left| \frac{\eta_{\pm}}{\eta_{00}} \right|^2 \quad (5)$$

$$\simeq 1 + 6Re(\epsilon'/\epsilon) \quad (6)$$

¹Unless noted, the years are given in published years.

deviates from 1 or not.

The superweak model [3] explained that a very weak unknown interaction that changes the strangeness by ± 2 brings in the phase. However, the superweak model cannot violate CP in the $K_L \rightarrow \pi\pi$ decay process because it cannot contribute to such a $\Delta S = \pm 1$ transition.

2.1 Advancement in Experimental Technologies

To measure the double ratio R , high statistics is required. This means that both a higher kaon flux and detectors capable to collect data with higher rates are needed.

2.1.1 Production Target

To get a higher kaon flux, the advancement of accelerators was essential, but there was also a change in production targets. In 1964, the experiment that first discovered CP violation with 35 $K_L \rightarrow \pi^+\pi^-$ events used an “internal target” in the accelerator ring as shown in Fig. 1. The target was a Be wire with 0.5 mm in diameter [4].

In 1969, at the CERN PS, the proton beam was extracted from the accelerator to bombard a 72-mm-thick tungsten target. About 400 $K_L \rightarrow \pi^+\pi^-$ events were collected [5], ten times more than in the first experiment.

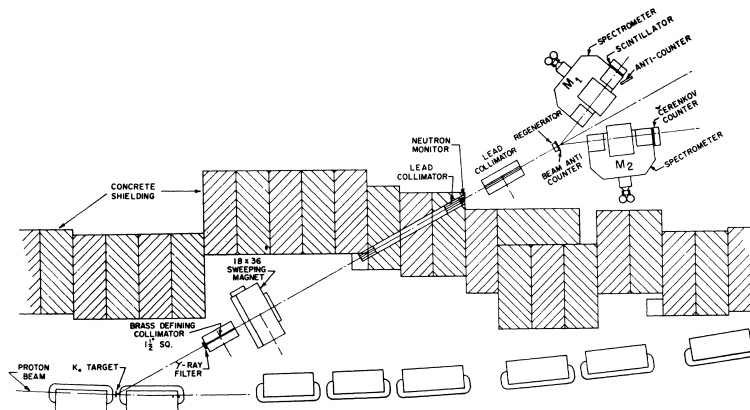


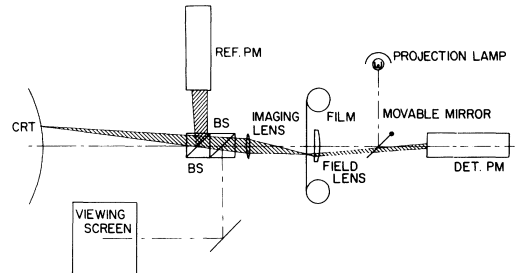
Figure 1: Plan view of the neutral kaon experiment at BNL AGS. For the experiment that discovered CP violation, the regenerator was removed, and a He bag was installed between the collimator and spectrometers [4]. © 2014 The American Physical Society.

2.1.2 Charged Spectrometers

There was also a change in detector technologies. The standard tracking devices in the 1960s were spark chambers. They had an advantage that only the tracks of interest can be made visible by applying HV pulses for triggered events. Mirrors were arranged to capture sparks in multiple spark chambers of each event in a single photograph. For the first CP

violation experiment, tracks in the photographs were scanned by human “scanners” with digitized angular encoders [4].

In 1969, the experiment at the CERN PS [5] used an automatic “Luciole Flying Spot Digitizer” which could scan 1000 frames per hour. This used a CRT instead of a mechanical system to move a bright light spot quickly across a film and record the intensity of light passing through the film with a phototube [6]. Figure 2 shows a similar spot scanner with a CRT, made by the Univ. of Michigan.



In the late 1960s, experiments started to move away from using films. Experiments at CERN and BNL used ferrite-core readout systems to read out spark positions and recorded them on tape directly [7, 8, 9]. This readout system allowed the BNL experiment to collect 9400 $K_{L,S} \rightarrow \pi^+\pi^-$ events, 300 times the first CP violation experiment.

Figure 2: A spot scanner using CRT as a moving light source. The light spot was controlled by a PDP-1 computer, and was focused onto the film, of which the local transparency was measured by a photomultiplier (DET. PM). ©2014 IEEE. Reprinted, with permission, from [6].

In the early 1970s, experiments started to use multi-wire proportional chambers (MWPC). For example, the experiment that observed the first $K_L \rightarrow \mu^+\mu^-$ decays [10] used MWPCs with 5000 wires that had a 2-mm wire spacing. With the same detector, the experiment collected 2 M $K_{L,S} \rightarrow \pi^+\pi^-$ events [11].

The geometry of spectrometers has also changed. The CP violation experiment in 1964 used a double-arm spectrometer with two sets of quadrupole magnets and spark chambers located at $\pm 22^\circ$ from the neutral beam line as shown in Fig. 1. This geometry was optimized for the 1.1-GeV/c average K_L momentum.

A later experiment at CERN [12] in 1965 used a forward spectrometer with one dipole magnet sandwiched between four spark chambers as shown in Fig. 3 to have a high acceptance for pions from K_L 's with the average momentum 11 GeV/c. It also had a Čerenkov counter between the downstream spark chambers for a particle identification. The forward spectrometer became the standard for the experiments that followed.

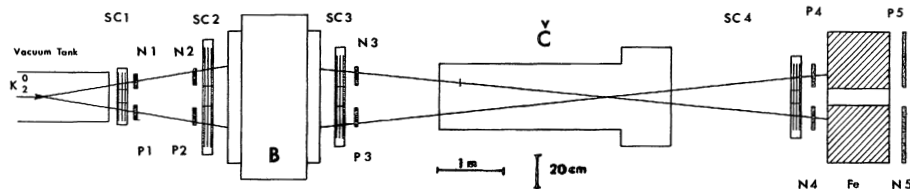


Figure 3: Plan view of an experimental apparatus at CERN which used a forward spectrometer. SC_i are spark chambers, N_i and P_i are scintillators, B is a bending magnet, and Č is a Čerenkov counter. Reprinted from [12]. Copyright 2014, with permission from Elsevier.

2.1.3 Photon Detectors

Let us now switch to the neutral $K_L \rightarrow \pi^0\pi^0$ mode. One of the questions after the discovery of CP violation was whether there was also the neutral counterpart of the $K_L \rightarrow \pi^+\pi^-$. The $K_L \rightarrow \pi^0\pi^0$ decay mode was far more difficult than the charged mode, because photons were not readily visible, and there was a large background from the $K_L \rightarrow \pi^0\pi^0\pi^0$ decay mode.

In 1968, an experiment at CERN [13] used a bubble chamber, 1.2 m in diameter and 1 m deep, filled with heavy liquid freon to collect events with 4 photons converted in the chamber. The experiment observed 24 events with 7.4 background events, and gave $BR(K_L \rightarrow \pi^0\pi^0) = (0.94 \pm 0.37) \times 10^{-3}$.

Also in 1968, an experiment at Princeton-Pennsylvania Accelerator [14, 15] used a spectrometer and “ γ chambers” surrounding the four sides of a 30 cm \times 30 cm K_L beam as shown in Fig. 4. A photon was converted in a 0.1 X_0 lead sheet placed on one side, and the resulting electron pair was momentum analyzed in a magnetic spectrometer. A wide gap spark chamber was used before the magnet to minimize multiple scatterings, and thin gap spark chambers were used to track the e^\pm pairs after leaving the magnet. The other three sides were covered with “ γ chambers” consisting of layers of steel plates and spark chambers to measure the hit positions of the other three photons. The hit timings were also recorded to measure the time-of-flight of K_L s with a peak momentum of 0.25 GeV/c bunched in a 1 ns width. The decay vertex was assumed to be along the photon momentum axis measured with the spectrometer to reconstruct the decay. The experiment observed 57 ± 9 events, and gave $BR(K_L \rightarrow \pi^0\pi^0) = (0.97 \pm 0.23) \times 10^{-3}$.

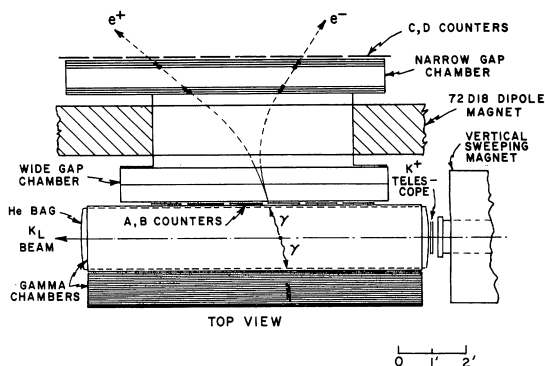


Figure 4: Plan view of the experimental apparatus that observed $K_L \rightarrow \pi^0\pi^0$ events. The K_L beam entered from the right, and photon detectors surrounded the *sides* of the beam [16]. © 2014 The American Physical Society.

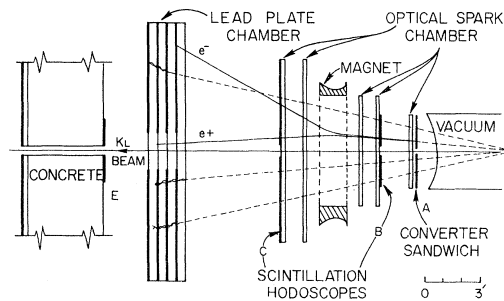


Figure 5: Schematic view of the experimental apparatus at BNL that was used to detect $K_L \rightarrow \pi^0\pi^0$ decays. Photon detectors were placed in the beam direction [17]. © 2014 The American Physical Society.

The same group then moved to BNL to measure $|\eta_{00}|/|\eta_{\pm}|$. The detector geometry was changed to have a higher acceptance for a higher mean K_L momentum (6 GeV/c), and to

detect both $\pi^+\pi^-$ and $\pi^0\pi^0$ modes. As shown in Fig. 5, a spectrometer and “ γ counters” were located in the beam-forward direction. Still it required one of the four photons to be converted in a $0.1X_0$ -thick converter, and the momenta of converted electron pairs to be measured. The $\pi^0\pi^0$ events were reconstructed basically with the same technique as the previous experiment, with the momentum of one photon, along with conversion positions, but not the energies, of other three photons. The experiment observed $124 \pm 11 K_L \rightarrow \pi^0\pi^0$ events with $3 \pm 3 K_L \rightarrow \pi^0\pi^0\pi^0$ background events [17].

2.1.4 Calorimeters

There was also an attempt to measure the energies and directions of *all* four photons with limited accuracies. An experiment at CERN [18] used two spark chamber systems with Al and brass plates, with a total thickness of $11.6 X_0$, as shown in Fig. 6. The number of sparks gave an energy resolution of 25% for 500 MeV electrons. The experiment observed about 200 $K_L \rightarrow \pi^0\pi^0$ events, and gave $BR(K_L \rightarrow \pi^0\pi^0) = (2.5 \pm 0.8) \times 10^{-3}$.

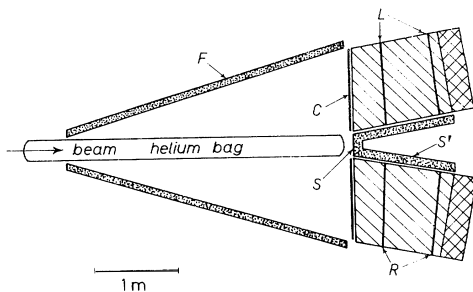


Figure 6: Plan view of the experiment apparatus at CERN (taken from [18]). Two spark chamber systems with radiators were used to measure conversion points, initial direction, and shower energy of each photon from $K_L \rightarrow \pi^0\pi^0$. With kind permission of Springer Science+Business Media.

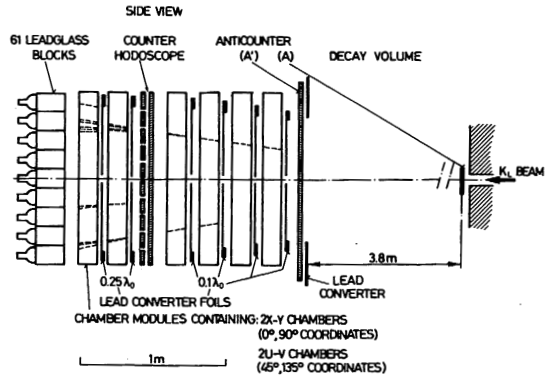


Figure 7: Plan view of the experiment apparatus at CERN using a lead glass array to measure the energy of photons from $K_L \rightarrow \pi^0\pi^0$. Spark chambers interleaved with converter foils were used to measure the conversion points and directions of two photons from the decay. Reprinted from [19]. Copyright 2014, with permission from Elsevier.

Another experiment at CERN [19] introduced a calorimeter consisting of 61 hexagonal lead-glass modules ($13 X_0$ long) to measure the energies of *all four* photons, as shown in Fig. 7. The energy resolution was $3.3\%/\sqrt{E_\gamma(\text{GeV})}$. The experiment also had spark chambers with lead foils to measure the directions of at least two photons to reconstruct the decay vertex. The pulse heights from the lead-glass and spark coordinates read out via ferrite cores were written on tape. The experiment collected 167 $K_L \rightarrow \pi^0\pi^0$ events, and gave $|\eta_{00}/\eta_{\pm}| = 1.00 \pm 0.06$.

2.2 Hard Wall

By 1973, the number of $K_L \rightarrow \pi^+\pi^-$ events reached 4200 [20]. However, the number of $K_L \rightarrow \pi^0\pi^0$ events was still about 200. The small statistics of $K_L \rightarrow \pi^0\pi^0$ events limited the accuracy of $Re(\epsilon'/\epsilon)$; the best results were $Re(\epsilon'/\epsilon) = -0.016 \pm 0.040$ [17], and $Re(\epsilon'/\epsilon) = 0.00 \pm 0.01$ [19], which were both consistent with 0. Experiments hit a hard wall.

In 1976, in his beautiful review, Kleinknecht wrote [21]

It is not easy to improve substantially the experimental precision. A decision between superweak and milliweak models of CP violation will therefore probably have to come from other experimental information outside the K^0 system.

Considering the difficulties that they had in the mid-1970s, such a view is not surprising.

What did kaon experiments do then? There were two major streams.

One was to measure the charge asymmetry of semi-leptonic $K_L \rightarrow \pi\ell\nu$ and $K_L \rightarrow \pi\mu\nu$ decays. The charge asymmetry, $\delta = (N^+ - N^-)/(N^+ + N^-)$, gives $2Re(\epsilon)$ where N^\pm is the number of observed $K_{\ell 3}$ decays with ℓ^\pm . These measurements required high statistics and a good control of systematic errors. For example, an experiment at CERN [22] collected 34M K_{e3} and 15M $K_{\mu 3}$ events, and measured $\delta_e = (3.65 \pm 0.17) \times 10^{-3}$ and $\delta_\mu = (3.23 \pm 0.26) \times 10^{-3}$.

The other stream was to measure the amplitudes of the regeneration of K_S from K_L interacting with materials. Although it looked irrelevant, this stream led to the measurements of $Re(\epsilon'/\epsilon)$ later.

2.3 Standard Model Prediction on the ϵ'/ϵ

In the 1970s, there were movements on the theoretical side. First, Kobayashi and Maskawa explained [23] that the phase which naturally comes in the mixing between 3 generations of quarks can explain the CP violation in the $K^0 - \bar{K}^0$ transition via a box diagram shown in Fig. 8(a). Second, in addition to a standard tree diagram shown in Fig. 8(b), a so-called penguin diagram for the $K_L \rightarrow \pi^+\pi^-$ decay shown in Fig. 8(c) was introduced by Ellis *et al.* [24] and Shifman *et al.* [25, 26]. The complex phase in the penguin diagram can violate CP in the decay process. Gilman and Wise predicted the value of $Re(\epsilon'/\epsilon)$ to be $(3 - 5) \times 10^{-3}$ with the Kobayashi-Maskawa model [27], whereas the superweak model predicted it to be 0. To measure the $Re(\epsilon'/\epsilon)$ with an accuracy of 1×10^{-3} , 30k $K_L \rightarrow \pi^0\pi^0$ events are needed, and systematic errors should be controlled to a 0.1% level. Although the predicted value was 10 times smaller than the values predicted by some other models, it gave a clear goal for experiments.

2.4 Precision Experiments

2.4.1 Early 1980s

In the early 1980s, a new generation of experiments started at BNL [28] and Fermilab (FNAL E617) [29]. Both experiments used dipole magnets and chambers (MWPCs for BNL, and drift chambers for Fermilab) to analyze the momentum of $\pi^+\pi^-$ tracks, as shown

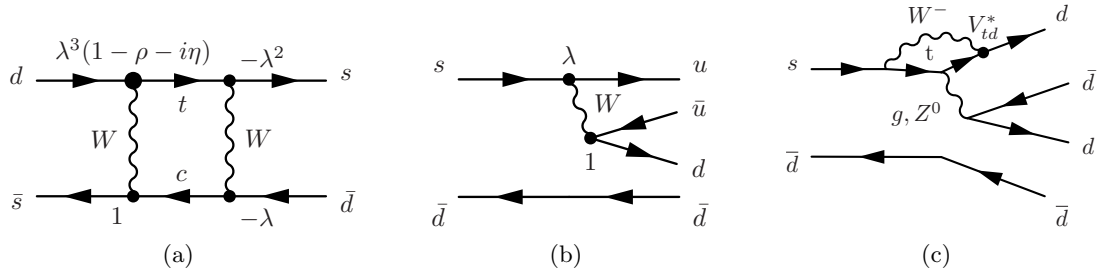


Figure 8: (a):Box diagram that introduces indirect CP violation in $K^0 - \bar{K}^0$ mixing. (b): Tree diagram for $K \rightarrow \pi\pi$. (c): Penguin diagram that can generate direct CP violation.

in Fig. 9. A thin lead sheet was placed upstream of the first chamber to convert one of the photons from the $\pi^0\pi^0$ decays, and to track the produced electron pairs. They both used lead glass arrays to measure the hit positions and energies of photons and electrons. The $K_L \rightarrow \pi e \nu$ events were rejected by comparing the energy deposit in the lead glass array and the track momentum. The $K_L \rightarrow \pi \mu \nu$ events were rejected by detecting muons passing through a steel wall located downstream of the calorimeter. Both experiments inserted carbon blocks in the K_L beam to regenerate K_S , but the techniques were different. In the BNL experiment, the regenerator was moved in and out to alternate between K_S and K_L runs. The Fermilab experiment had two K_L beams, and moved the regenerator between the two beams to observe K_L and K_S decays simultaneously, which cancels various systematical effects. Another difference was the proton and kaon momentum; the BNL experiment used 28-GeV protons to produce 7-14 GeV/c kaons, while the Fermilab experiment used 400-GeV protons to produce kaons with the mean momentum around 70–90 GeV/c. The BNL experiment collected 1120 $K_L \rightarrow \pi^0\pi^0$ events and gave $Re(\epsilon'/\epsilon) = 0.0017 \pm 0.0082$. The Fermilab experiment collected 3150 $K_L \rightarrow \pi^0\pi^0$ events and gave $Re(\epsilon'/\epsilon) = -0.0046 \pm 0.0058$. Although both results were consistent with 0, it became clear that using higher energy kaons was more advantageous because of the higher acceptance and the better energy resolution for photons.

It is worth noting that the Fermilab E617 was the cornerstone for the Fermilab ϵ'/ϵ experiments that followed. The experiment introduced a double beam technique, using a regenerator to observe K_L and K_S decays simultaneously to suppress systematic errors. This double-beam technique was actually inherited from Fermilab E226 and E486 which studied regeneration on electrons [30] and coherent regeneration amplitudes on various nuclei [31], respectively.

2.4.2 Fermilab E731

In the mid-1980s, Fermilab E731 was built. It used 800 GeV protons to produce two K_L beams with the average energy of 70 GeV. An improved B_4C regenerator alternated between the two beams every spill. Four drift chambers were built for a better position resolution, and a lead glass array was used as an electromagnetic calorimeter. Initially, for the $\pi^0\pi^0$ run, a 0.1- X_0 -thick lead sheet was inserted at the end of a decay volume to convert one

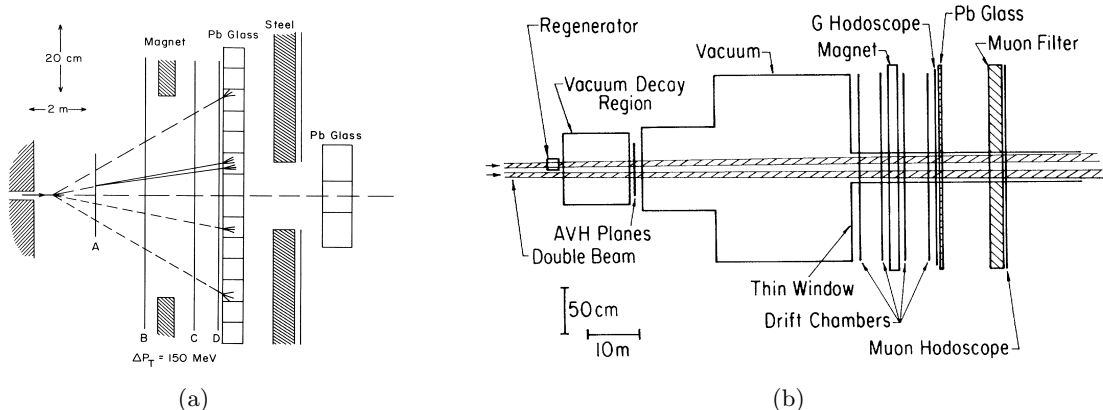


Figure 9: (a): Schematics of the $Re(\epsilon'/\epsilon)$ experimental apparatuses at BNL (taken from [28]), and (b): Fermilab E617 (taken from [29]). Fermilab E617 used two beams to observe K_L and K_S decays simultaneously. © 2014 The American Physical Society.

of the photons for tracking, just as the past experiments. A dipole magnet located just downstream of the lead sheet split the electron pairs. Its field was tuned such that the downstream spectrometer would focus the pair on to the lead glass calorimeter, as shown in Fig. 10. However, requiring a photon conversion imposed a limit on the statistics; only 30% of the $\pi^0\pi^0$ decays had converted electron pairs, and the $\pi^+\pi^-$ and $\pi^0\pi^0$ events had to be collected in separate runs because the lead sheet had to be removed for the $\pi^+\pi^-$ run to minimize multiple scatterings.

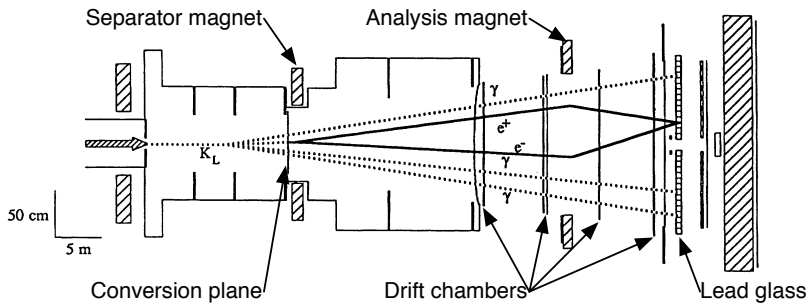


Figure 10: Plan view of the Fermilab E731 apparatus. Two beams were aligned vertically. Initially, for the $K_L \rightarrow \pi^0\pi^0$ decay mode, one of the photons were required to be converted.

After some studies, the experiment decided to break the 30 years of tradition of converting photons. For the last part of the experiment, it ran without the lead sheet, and collected 4 photons without converting them,² and also took $\pi^+\pi^-$ and $\pi^0\pi^0$ modes simultaneously for the first time. This big step was made possible by two technological developments. One

²CERN NA31 experiment triggered on $2\pi^0$ events with a hodoscope in a liquid Ar calorimeter.

was a second-level trigger to count the number of clusters in the calorimeter [32] which reduced the trigger rate by a factor 10 by collecting only 4 and 6 clusters. The other was a FASTBUS-based data acquisition system which reduced the dead time by a factor 10, from 5 ms to 0.5 ms.

At the end, Fermilab E731 collected 410 k $K_L \rightarrow \pi^0\pi^0$ events and 327 k $K_L \rightarrow \pi^+\pi^-$ events, and gave $Re(\epsilon'/\epsilon) = (7.4 \pm 5.2(\text{stat}) \pm 2.9(\text{syst})) \times 10^{-4}$ [33]. Compared to E617, it reduced the overall error by a factor 14 with 130 times more $K_L \rightarrow \pi^0\pi^0$ events.

The Fermilab result was only 1.2σ away from 0, and still consistent with 0, whereas its competitor, CERN NA31, gave $Re(\epsilon'/\epsilon) = (20 \pm 7) \times 10^{-4}$ [34] which was 3σ away from 0. There were intense arguments between the two experiments. CERN NA31 used a moving production target for K_S runs to make the K_L and K_S decay vertex distributions similar. The experiment claimed that this method made the analysis less dependent on Monte Carlo simulations. Fermilab E731 argued that even with different decay vertex distributions between K_L and regenerated K_S , the geometrical acceptances obtained with Monte Carlo simulations can be checked with high-statistics decay modes such as $K_L \rightarrow \pi e \nu$ and $K_L \rightarrow \pi^0\pi^0\pi^0$. Also, it argued that it is more important to collect K_L and K_S data simultaneously with the same detector, rather than to take $\pi^+\pi^-$ and $\pi^0\pi^0$ modes simultaneously, because efficiencies of charged and neutral mode detectors have different rate dependences. These arguments, however, could not solve the discrepancy between the two experimental results. At the end, both groups decided to build new experiments, CERN NA48, and Fermilab KTeV-E832, to improve the accuracy and precision by another order of magnitude. In this paper, I will concentrate on KTeV-E832, because CERN NA48 will be covered in detail by M. Sozzi [35].

2.4.3 Fermilab KTeV-E832

Fermilab KTeV built a new beam line with a better collimation scheme to make a cleaner beam with less halo neutrons even with a higher proton intensity. Figure 11(a) shows the plan view of the KTeV detectors. The new regenerator was made of fully active scintillators to suppress backgrounds from non-coherent regenerations. A new large spectrometer magnet with a uniform field was made for the $\pi^+\pi^-$ decays. A new electromagnetic calorimeter shown in Fig. 11(b), covering $1.9 \text{ m} \times 1.9 \text{ m}$, was built with pure CsI crystals $27 X_0$ long, to have a better energy resolution. To improve the position resolution, 2.5-cm-square crystals were used in the central $1.2 \text{ m} \times 1.2 \text{ m}$ region, and 5.0-cm-square crystals in the outer region. The scintillation light from the crystals were read out by phototubes and digitized right behind the phototubes every 19 ns to minimize electric noise, record the pulse shape, and to supply hit information for counting the number of clusters. The energy resolution was less than 1% for most of the energy range, reaching about 0.45%, which was the best resolution for the calorimeter of this size. A new data acquisition system used a matrix of memories to buffer events during spill³ and to distribute the events evenly to 36 120-MIPS CPUs (fast in those days) to reconstruct all the events for online filtering.

³The dead time of the trigger and data acquisition system was only 10 μs , 1/50 of that of E731. It could accept 8 kbyte events coming at 20 kHz for 20 s spill with a 60 s cycle.

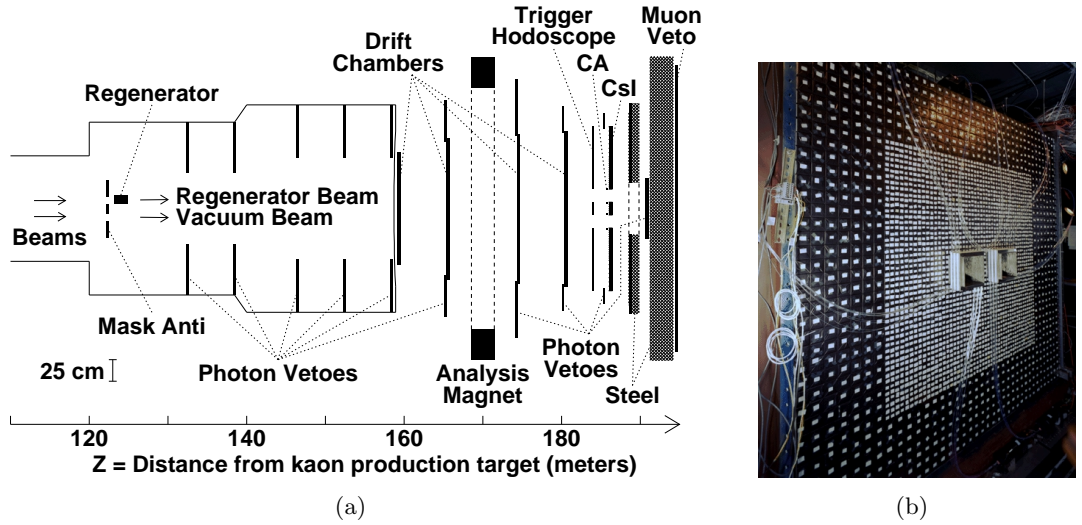


Figure 11: (a) Plan view of the Fermilab KTeV apparatus (taken from [37]). © 2014 The American Physical Society. (b) KTeV CsI electromagnetic calorimeter.

Figure 12 shows the decay vertex distributions for the $\pi^+\pi^-$, $\pi^0\pi^0$, and other high statistics decay modes. The number of $K_L \rightarrow \pi^0\pi^0$ events was 6M. The data and Monte Carlo distributions agreed well, and the systematic errors on the $Re(\epsilon'/\epsilon)$ due to acceptance correction were 0.57×10^{-4} for charged modes and 0.48×10^{-4} for neutral modes. The first result based on 20% of data taken in 1996-1997 runs was $Re(\epsilon'/\epsilon) = (28.0 \pm 4.1) \times 10^{-4}$ [36], 7σ away from 0, and the final result with the full data was $Re(\epsilon'/\epsilon) = (19.2 \pm 1.1(\text{stat}) \pm 1.8(\text{syst})) \times 10^{-4} = (19.2 \pm 2.1) \times 10^{-4}$ [37].

2.5 Conclusion on the ϵ'/ϵ

CERN NA48 gave $Re(\epsilon'/\epsilon) = (14.7 \pm 2.2) \times 10^{-4}$ based on all data [38]. The result averaged by PDG is $(16.6 \pm 2.3) \times 10^{-4}$ [39], 7.2σ away from 0. CERN NA48 and Fermilab KTeV-E832 have both clearly established that the $Re(\epsilon'/\epsilon)$ is not 0, thereby rejecting the Superweak model, and supported the Kobayashi-Maskawa model.

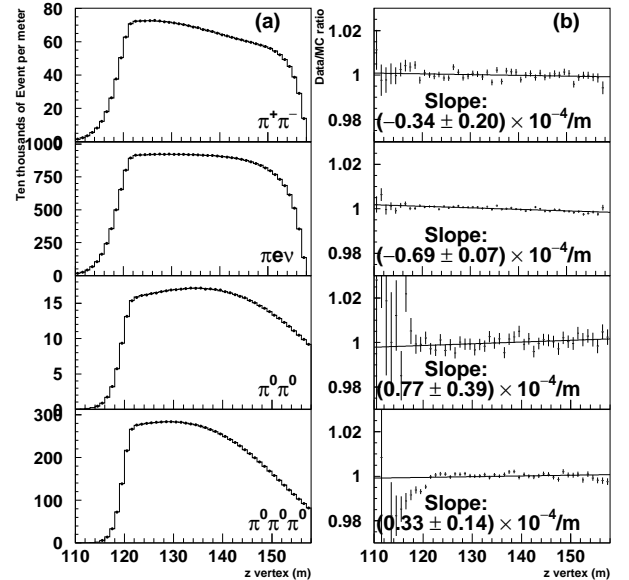


Figure 12: (a) Decay vertex distributions of $K_L \rightarrow \pi^+\pi^-$, $K_L \rightarrow \pi\pi\nu$, $K_L \rightarrow \pi^0\pi^0$, and $K_L \rightarrow \pi^0\pi^0\pi^0$ decays for the data (dots) and MC (histogram). (b) The data-to-MC ratios are fit to a line (taken from [37]). © 2014 The American Physical Society.

2.6 Looking Back

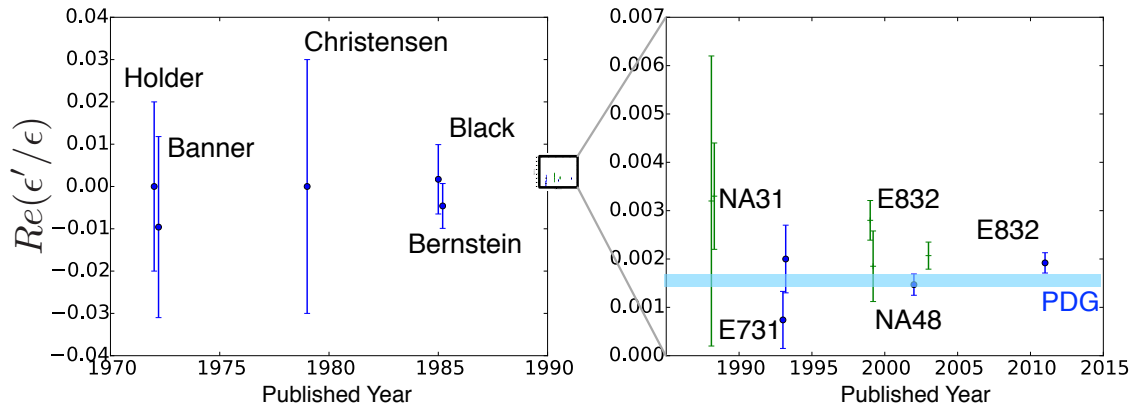


Figure 13: The results of $Re(\epsilon'/\epsilon)$ vs. published year. The horizontal band shows the PDG average [39].

Figure 13 shows the history of results on the $Re(\epsilon'/\epsilon)$. The plot showing the final results is minuscule in the scale of early experiments. Figure 14 shows the error on the $Re(\epsilon'/\epsilon)$ as a function of the number $K_L \rightarrow \pi^0\pi^0$ events (N). The error is clearly proportional to $1/\sqrt{N}$. This means that the systematic errors were also reduced accordingly with statistical errors. All these improvements in statistics and precision were made not only by the beam power. Beam line design, chamber technology, photon measurement technology, trigger and data acquisition systems, and even magnetic tape technology had to be improved along with it, and behind them were people's innovative ideas, deep thinking, and many years of hard work.

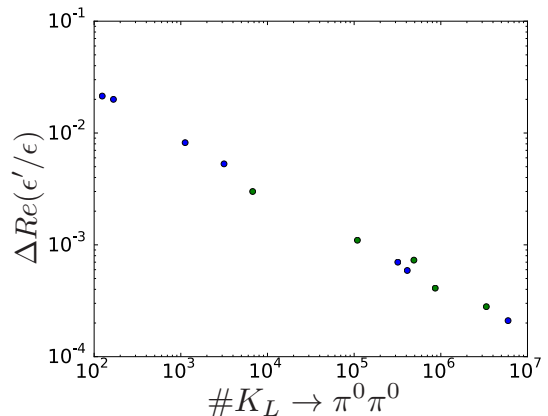


Figure 14: The errors on $Re(\epsilon'/\epsilon)$ are shown as a function of the number of $K_L \rightarrow \pi^0\pi^0$ events for the past experiments.

3 Quest for $K \rightarrow \pi\nu\bar{\nu}$

With the $Re(\epsilon'/\epsilon)$ results and the observation of CP violation in B decays, the Kobayashi-Maskawa model was determined to be the source of CP violations that had been observed in *laboratories*, and became a solid piece in the standard model. However, the effect of this CP violation mechanism is still too small to explain the baryon – antibaryon asymmetry in

the universe. There should be new physics beyond the standard model that violates CP . After the establishment of $Re(\epsilon'/\epsilon) \neq 0$, kaon experiments changed their focus to search for new physics beyond the standard model. To search for a small sign of new physics, there are two important points. First, the background has to be small, and second, it has to be known with a small error. Here, in addition to backgrounds caused by experimental techniques such as misidentifying particles or mis-measurements, background decays caused by the standard model itself should also be well known.

3.1 Physics of $K \rightarrow \pi\nu\bar{\nu}$

The decay modes that have small and well-known branching ratios are $K_L \rightarrow \pi^0\nu\bar{\nu}$ and $K^+ \rightarrow \pi^+\nu\bar{\nu}$. These decay modes proceed through a penguin diagram as shown in Fig. 15. In the standard model, the major contribution comes from a diagram with a top quark in the loop. The branching ratios predicted by the standard model are small: $BR(K_L \rightarrow \pi^0\nu\bar{\nu}) = 2.4 \times 10^{-11}$, and $BR(K^+ \rightarrow \pi^+\nu\bar{\nu}) = 7.8 \times 10^{-11}$ [40]. Also, theoretical uncertainties are only about 2 – 4%. The current errors are dominated by the errors of the known CKM parameters, and those will be reduced in the upcoming B factory experiments.

New physics can contribute to these decays by having new physics particles in the loop. It can then change the branching ratios from the values predicted by the standard model. The $K_L \rightarrow \pi^0\nu\bar{\nu}$ decay is sensitive to new physics that breaks CP symmetry, because K_L is mostly CP odd, and the $\pi^0\nu\bar{\nu}$ state is CP even.

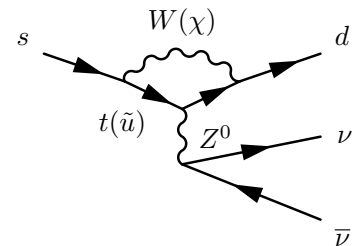


Figure 15: Penguin diagram of the $K \rightarrow \pi\nu\bar{\nu}$ decay. In standard model, top quark is dominant in the loop. New physics particles can enter the loop and have additional contribution.

3.2 History of $K^+ \rightarrow \pi^+\nu\bar{\nu}$ Experiments

Let us first start from the charged $K^+ \rightarrow \pi^+\nu\bar{\nu}$ decay. The signature of the decay is a single π^+ decaying from a K^+ . Major backgrounds are $K^+ \rightarrow \mu^+\nu$ decay where the μ^+ is misidentified as π^+ , and $K^+ \rightarrow \pi^+\pi^0$ decay where the two photons from the π^0 are missed.

The search for $K^+ \rightarrow \pi^+\nu\bar{\nu}$ also has a long history, and dates back to 1970 [41]. The $K^+ \rightarrow \pi^+\nu\bar{\nu}$ events were first observed by BNL E787, and its branching ratio was measured by the E787 and E949 experiments. Figure 16(a) shows the detector of BNL E949. The experiment stopped the K^+ beam in a target, and looked for a single π^+ coming out from the target. Stopping the K^+ simplifies the kinematics in reconstruction because the lab frame and the center of mass frame are the same. The momentum of the π^+ is measured with a solenoid magnetic and a central drift chamber. The energy deposit and the range of the π^+ were measured in a stack of scintillators (range counter) for identifying pions. In addition, the $\pi^+ \rightarrow \mu^+ \rightarrow e^+$ decay chain was traced by recording wave forms in the range counter to further identify pions.⁴ The detector was surrounded by photon veto counters

⁴This technique was first used in KEK E10 experiment to search for the $K^+ \rightarrow \pi^+\nu\bar{\nu}$ decay [42].

to suppress the background from $K^+ \rightarrow \pi^+\pi^0$ decays. Figure 16(b) shows the scatter plot of the energy deposit and the range of π^+ events observed by BNL E787 and E949. The experiments found 7 events in total, and gave $BR(K^+ \rightarrow \pi^+\nu\bar{\nu}) = (1.73^{+1.15}_{-1.05}) \times 10^{-10}$ [43].

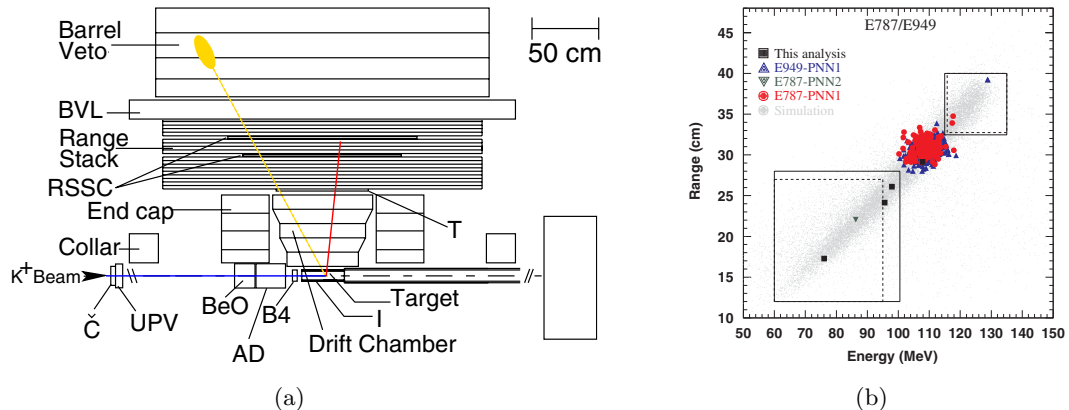


Figure 16: (a) Schematic side view of the upper half of the BNL E949 detector. (b) Range vs kinetic energy of all events passing all other cuts observed by the BNL E787 and E949 experiments [43]. © 2014 The American Physical Society.

Currently, CERN NA61 is preparing a new experiment to collect 45 $K^+ \rightarrow \pi^+\nu\bar{\nu}$ standard model events per year. It uses high energy decay-in-flight K^+ s to minimize hadron interactions in the beam line, and uses Čerenkov counters to identify pions and kaons. More details of the NA61 is covered by M. Sozzi [35].

3.3 History of $K_L \rightarrow \pi^0\nu\bar{\nu}$ Experiments

Let us next move to the neutral $K_L \rightarrow \pi^0\nu\bar{\nu}$ decay. Although the $K_L \rightarrow \pi^0\nu\bar{\nu}$ decay mode is theoretically clean, it is challenging experimentally. One cannot trigger on the incoming K_L because it is neutral, and the only observable particles are the two photons from the π^0 decay. The initial K_L momentum and its decay vertex is unknown, making the signal selection difficult. In addition, there is a major background from the $K_L \rightarrow \pi^0\pi^0$ decay mode if two of the four photons from the decay are missed.

The first experimental upper limit on the branching ratio was $BR(K_L \rightarrow \pi^0\nu\bar{\nu}) < 7.6 \times 10^{-3}$ (90% CL) [44], based on the Cronin's old result on $K_L \rightarrow \pi^0\pi^0$ [45].

The first dedicated data was taken by KTeV E799-II, a rare-kaon experiment at Fermilab. It had a one-day special run to look for events with only 2 photons which decayed from the π^0 in $K_L \rightarrow \pi^0\nu\bar{\nu}$ decay, and gave an upper limit, $BR(K_L \rightarrow \pi^0\nu\bar{\nu}) < 1.6 \times 10^{-6}$ (90% CL) [46].

The KTeV E799-II also looked for the π^0 Dalitz decay. Using the e^+e^- tracks from the Dalitz decay, the decay vertex was reconstructed, the $m_{ee\gamma}$ was required to be consistent with the π^0 mass, and the π^0 was required to have a transverse momentum $P_T > 0.16$ GeV/c. Based on no observed events, the experiment gave $BR(K_L \rightarrow \pi^0\nu\bar{\nu}) < 5.9 \times 10^{-7}$ (90% CL) [47]. Although the Dalitz decay can provide tight kinematical constraints, it has

less sensitivity than the experiments with $\pi^0 \rightarrow \gamma\gamma$ decays, because the $BR(\pi^0 \rightarrow e^+e^-\gamma)$ is only 1.2%, and the acceptance for the e^+e^- pair is small due to its small opening angle.

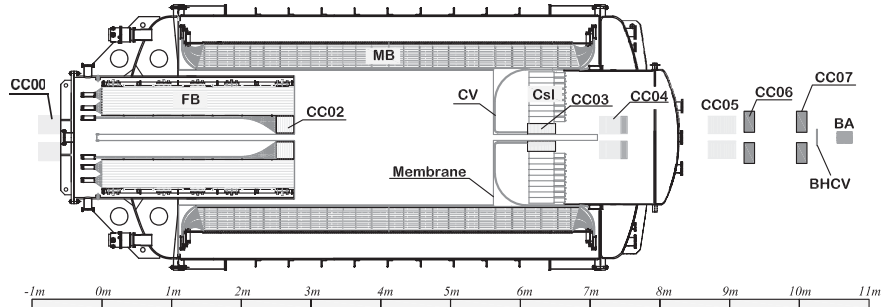


Figure 17: Schematic view of the KEK E391a detector (taken from [48]). © 2014 The American Physical Society.

The first dedicated experiment for the $K_L \rightarrow \pi^0\nu\bar{\nu}$ decay was KEK E391a experiment. A K_L beam with the average momentum of 2 GeV/c was made by bombarding a target with 12 GeV protons.

As shown in Fig. 17, the detector consists of an electromagnetic calorimeter to detect two photons from the π^0 , and a hermetic photon veto system surrounding a decay volume to suppress the $K_L \rightarrow \pi^0\pi^0$ background. The calorimeter was made of 7-cm square and 30-cm long pure CsI crystals stacked inside a cylinder with 1 m radius. The surfaces of these detectors were covered by plastic scintillators to veto charged particles. All of these detectors were housed inside a vacuum tank. The neutral beam had to be in vacuum to suppress π^0 s produced by neutrons interacting with residual gas, and thus required a beam pipe. If the detectors were located outside the beam pipe, low energy photons could be absorbed in the beam pipe, and the $K_L \rightarrow \pi^0\pi^0$ background would increase. The solution was to minimize such dead material by placing most of the detectors inside effectively a large “beam pipe”. The calorimeter had a hole at the center for the beam to pass through. In downstream, another photon veto counter was placed in the beam to veto photons escaping through the hole.

Figure 18 shows the scatter plot of decay vertex and the transverse momentum (P_T) of π^0 s. The decay vertex and P_T were reconstructed by assuming that the two photons from a π^0 originated at the center of the beam area. Based on no events in the signal region, the

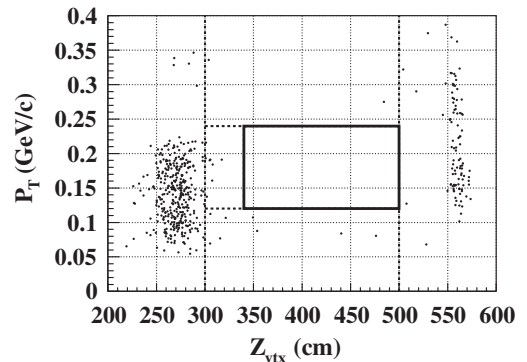


Figure 18: Scatter plot of the reconstructed P_T vs the Z position of the events that passed all other cuts observed by KEK E391a experiment (taken from [48]). The solid rectangle indicates the signal region.

experiment lowered the upper limit to $BR(K_L \rightarrow \pi^0 \nu \bar{\nu}) < 2.6 \times 10^{-8}$ (90% CL) [48].

3.4 J-PARC KOTO Experiment

A new $K_L \rightarrow \pi^0 \nu \bar{\nu}$ experiment, called KOTO, is starting up at the J-PARC laboratory in Japan. It utilizes a high intensity 30-GeV proton beam to achieve a sensitivity close to the branching ratio predicted by the standard model [49]. The protons extracted from the Main Ring hit a common target shared by multiple experiments. A neutral beam line is extracted at 16° from the proton beam line. A new pair of collimators were designed to suppress neutrons in the beam halo. The vacuum tank and photon veto detectors used at the KEK E391a were moved to J-PARC. The electromagnetic calorimeter was replaced with the pure CsI crystals used for the Fermilab KTeV experiments. With their small cross-sections (2.5-cm-square crystals in the $1.2 \text{ m} \times 1.2 \text{ m}$ region, and 5-cm-square crystals in the outer region), it has a better γ /neutron identification, and it can suppress backgrounds caused by two photons hitting the calorimeter together, which is another mechanism of missing a photon. The energy resolution is also improved by their longer length, 50 cm ($27X_0$). The charged veto counter covering the upstream side of the calorimeter was replaced with two layers of plastic scintillators. Each plane is only 3 mm thick to suppress halo neutrons interacting in the counter. The photon veto detector covering the upstream end of the decay volume was replaced with CsI crystals to improve the veto efficiency and to detect beam-halo neutrons. A new photon veto detector was placed in the beam downstream of the calorimeter to veto photons escaping through the beam hole in the calorimeter. The detector was made of modules consisting of a lead converter and an aerogel Čerenkov counter to have a low veto inefficiency (10^{-3}) for photons even under full beam intensity. The signals from all the detector components are digitized with flash ADCs. They are used to record the waveforms to identify signals in a high-rate environment, and to produce trigger signals based on the digitized information.

The KOTO experiment started its first physics run in May 2013. Although the run was terminated after 100 hours of data taking due to a radiation accident in the experimental hall, it is pursuing physics analysis intensively.⁵ After the J-PARC Hadron Experimental Facility recovers from the accident, KOTO is planning to install a new photon veto detector, increase the beam intensity, and start high-sensitivity runs.

3.5 Prospect of $K \rightarrow \pi \nu \bar{\nu}$ experiments

Figure 19 shows the predictions of the branching ratios of $K^+ \rightarrow \pi^+ \nu \bar{\nu}$ and $K_L \rightarrow \pi^0 \nu \bar{\nu}$ by various theoretical models. In the next few years, the CERN NA61 and J-PARC KOTO experiments will explore this large unexplored region.

4 Summary

Figure 20 shows my view of how the kaon experiments have evolved in the past 50 years. After the first series of CP violation experiments in the 1960s, kaon experiments have once

⁵The first result was presented at the CKM2014 Conference at Vienna in September 2014.

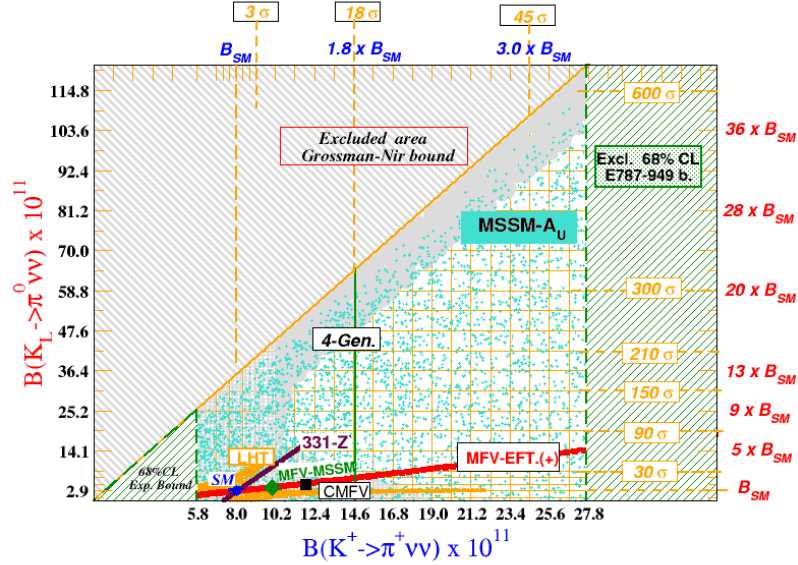


Figure 19: Branching ratios of $K_L \rightarrow \pi^0 \nu \bar{\nu}$ vs $K^+ \rightarrow \pi^+ \nu \bar{\nu}$ predicted by various theoretical models (taken from [50]).

moved on to high precision experiments to measure the charge asymmetry in semileptonic decays and K_S regeneration amplitudes. The experimental technologies and knowledge accumulated then later became the foundations of the modern $Re(\epsilon'/\epsilon)$ experiments which established the non-zero value. The stream of high-statistics experiments have also moved onto rare K decay experiments which I could not cover in my talk. These two streams are now recombined to the new $K \rightarrow \pi \nu \bar{\nu}$ experiments to search for physics beyond the standard model. Now that we are finally entering an unexplored territory, we should be open to any new signs that may appear.

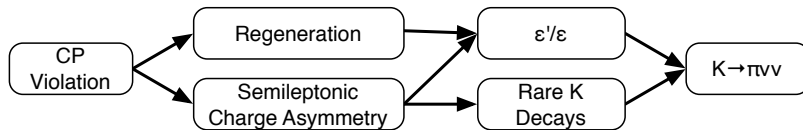


Figure 20: Evolution of kaon experiments since the discovery of CP violation.

5 Acknowledgements

I would like to thank the conference organizer for inviting me to give this review talk, and thereby giving me a chance to study the great works of past which are the foundations

of the current experiments. This work was supported by JSPS KAKENHI Grant Number 23224007.

References

- [1] J. H. Christenson, J. W. Cronin, V. L. Fitch and R. Turlay, *Phys. Rev. Lett.* **13** (1964) 138.
- [2] T. D. Lee and C.S. Wu, *Ann. Rev. Nucl. Sci.* **16**, 511 (1966).
- [3] L. Wolfenstein, *Phys. Rev. Lett.* **13**, 562 (1964).
- [4] J. H. Christenson *et al.*, *Phys. Rev.* **140**, B74 (1965).
- [5] A. Böhm *et al.*, *Nucl. Phys.* **B9**, 605 (1969).
- [6] W. A. Wenzel, *IEEE Trans. Nucl. Sci.* **13**, 34 (1966).
- [7] H. Faissner *et al.*, *Phys. Lett.* **30B**, 204 (1969).
- [8] D. A. Jensen *et al.*, *Phys. Rev. Lett.* **23**, 615 (1969).
- [9] D. Fryberger *et al.*, *IEEE Trans. Nucl. Sci.* **15**, 579 (1968).
- [10] W. C. Carithers *et al.*, *Phys. Rev. Lett.* **30**, 1336 (1973).
- [11] W. C. Carithers *et al.*, *Phys. Rev. Lett.* **34**, 1244 (1975).
- [12] X. De Bouard *et al.*, *Phys. Lett.* **15**, 58 (1965).
- [13] I. A. Bugadov *et al.*, *Phys. Lett.* **28B**, 215 (1968).
- [14] M. Banner *et al.*, *Phys. Rev. Lett.* **21**, 1107 (1968).
- [15] M. Banner *et al.*, *Phys. Rev.* **188**, 2033 (1969).
- [16] M. Banner *et al.*, *Phys. Rev. Lett.* **21**, 1103 (1968).
- [17] M. Banner *et al.*, *Phys. Rev. Lett.* **28**, 1597 (1972).
- [18] J.-M. Gaillard *et al.*, *Nuov. Cim. A Ser. 10*, **59**, 453 (1969).
- [19] M. Holder *et al.*, *Phys. Lett.* **40B**, 141 (1972).
- [20] R. Messner *et al.*, *Phys. Rev. Lett.* **30**, 876 (1973).
- [21] K. Kleinknecht, *Ann. Rev. Nuc. Sci.* **26**, 1 (1976).
- [22] C. Geweniger *et al.*, *Phys. Lett.* **48B**, 483 (1974).
- [23] M. Kobayashi and K. Maskawa, *Prog. Theo. Phys.* **49**, 652 (1973).

- [24] J. Ellis, M.K. Galliard, and D.V. Nanopoulos, Nucl. Phys. **B 109**, 213 (1976).
- [25] A. I. Vainshtein *et al.*, JETP Lett. **22**, 55 (1975).
- [26] M. A. Shifman *et al.*, Nucl. Phys. **B120**, 316 (1977).
- [27] F. J. Gilman and M. B. Wise, Phys. Rev. D **20**, 2392 (1979). It was later improved in F. J. Gilman and J. S. Hagelin, Phys. Lett. **133B**, 443 (1983).
- [28] J. K. Black *et al.*, Phys. Rev. Lett. **54**, 1628 (1985).
- [29] R. H. Bernstein *et al.*, Phys. Rev. Lett. **54**, 1631 (1985).
- [30] W. R. Molzon *et al.*, Phys. Rev. Lett. **41**, 1213 (1978).
- [31] A. Gsponer *et al.*, Phys. Rev. Lett. **42**, 13 (1979).
- [32] M. Asner *et al.*, Nucl. Inst. Meth. bf **A291**, 577 (1990).
- [33] L. K. Gibbons *et al.*, Phys. Rev. Lett. **70**, 1203 (1993).
- [34] G. D. Barr *et al.*, Phys. Lett. B **317**, 233 (1993).
- [35] M. Sozzi, in the same volume.
- [36] A. Alavi-Harati *et al.*, Phys. Rev. Lett. **83**, 22 (1999).
- [37] E. Abouzaid *et al.*, Phys. Rev. D **83**, 092001 (2011).
- [38] J. R. Batley *et al.*, Phys. Lett. B **544**, 97 (2002).
- [39] K. A. Olive *et al.*(Particle Data Group), Chin. Phys. C, **38**, 090001 (2014).
- [40] J. Brod, M. Gorbahn and E. Stamou, Phys. Rev. D **83**, 034030 (2011).
- [41] J. H. Klems *et al.*, Phys. Rev. Lett. **24**, 1086 (1970).
- [42] Y. Asano *et al.*, Phys. Lett. B **107**, 159 (1981).
- [43] A. V. Artamonov *et al.*, Phys. Rev. D **79**, 092004 (2009).
- [44] L. S. Litternberg, Phys. Rev. D **39**, 3322 (1989).
- [45] J. W. Cronin *et al.*, Phys. Rev. Lett. **18**, 25 (1967).
- [46] J. Adams *et al.*, Phys. Lett. B **447**, 240 (1999).
- [47] A. Alavi-Harati *et al.*, Phys. Rev. D **61**, 072006 (2000).
- [48] J. K. Ahn *et al.*, Phys. Rev. D **81**, 072004 (2010).
- [49] J. Comfort *et al.*, <http://koto.kek.jp/pub/p14.pdf>.
- [50] F. Mescia and C. Smith, <http://www.lnf.infn.it/wg/vus/content/Krare.html>.